

Optical long baseline intensity interferometry : prospects for stellar physics

Jean-Pierre Rivet · Farrokh Vakili ·
Olivier Lai · David Vernet · Mathilde
Fouché · William Guerin · Guillaume
Labeyrie · Robin Kaiser

Submitted to Experimental Astronomy, January 31st, 2018

Abstract More than sixty years after the first intensity correlation experiments by Hanbury Brown and Twiss, there is renewed interest for intensity interferometry techniques for high angular resolution studies of celestial sources. We report on a successful attempt to measure the bunching peak in the intensity correlation function for bright stellar sources with 1 meter telescopes (I2C project). We propose further improvements of our preliminary experiments of spatial interferometry between two 1 m telescopes, and discuss the possibility to export our method to existing large arrays of telescopes.

Keywords Temporal and spatial photon bunching · micro-arc-second interferometry · in the optical wavelengths

1 Introduction: historical background and revival

Like classical amplitude interferometry, intensity interferometry is a high-resolution observing technique used in astronomy to extend the angular resolution far beyond the classical resolution limit of single aperture instruments (optical or radio telescopes).

The principle underlying intensity interferometry is to monitor the space and/or time correlations of the electromagnetic wave intensity fluctuations in a given, limited bandwidth.

This idea was first proposed by Robert Hanbury Brown and theorized by Richard Twiss in the early 1950', in order to estimate the sizes of radio-sources beyond the resolution capabilities of classical amplitude radio-interferometry.

Jean-Pierre Rivet · Farrokh Vakili · Olivier Lai · David Vernet

¹Université Côte d'Azur, OCA, CNRS, Lagrange, France

E-mail: Jean-Pierre.Rivet@oca.eu

Mathilde Fouché · William Guerin · Guillaume Labeyrie · Robin Kaiser

²Université Côte d'Azur, CNRS, Institut de Physique de Nice, France

This method was first tested on-sky by Hanbury Brown et al (1952) to determine the size of “Cygnus A” and “Cassiopea A” radio-sources. Independently, similar diameter values were obtained for these objects by classical amplitude interferometry by Mills (1952) and Smith (1952).

In order to extend their concept to the optical domain, Hanbury Brown and Twiss (HBT hereafter) first performed successful laboratory experiments on an artificial light source (Mercury arc lamp) with two photomultiplier tubes (Hanbury Brown and Twiss, 1956a). They demonstrated further the efficiency of their method in real, less than ideal atmospheric conditions, by measuring the diameter of the star Sirius with a prototype intensity interferometer involving two 1.56 m searchlight projectors used as photons collectors (Hanbury Brown and Twiss, 1956b).

This first preliminary experiment paved the way for a more ambitious experiment : the Narrabri stellar intensity interferometer (NSII). The experimental setup involved two 6.5 m reflectors on a circular track with diameter 188 m. This configuration allowed adjusting the interferometric baselines up to 188 m, whilst maintaining the baseline projection constant (Hanbury Brown et al, 1967a,b; Hanbury Brown, 1968). From 1964 to 1972, the NSII has been used to perform ambitious experiments and led to the first consistent catalog of diameter measurements for 32 stars from spectral type O5 to F8 (Hanbury Brown et al, 1974a).

Classical amplitude interferometry requires to control the time-dependent sidereal optical path difference (OPD) between the arms of the interferometer with accuracies better than the wavelength of the radiation under consideration, on sub-millisecond time scales. This constraint is not considered as a challenge anymore, at least for long wavelengths (radio-interferometers) or in the optical domain for baselines of at most a few hundred meters, like for VLTI, CHARA and NPOI astronomical interferometers (Gomes et al, 2017; Mourard et al, 2015; Garcia et al, 2016). In the latter case, high precision optical delay lines are required to transport coherently the light signal from individual telescopes to the focal plane of the interferometer. For amplitude interferometry with very long baselines at short wavelengths (optical domain), the OPD compensation is still a challenging issue.

On the contrary, intensity interferometry only requires OPD control with accuracies given by the bandwidth of the bandpass filter (equivalently, by the time resolution of the acquisition chain), rather than by the wavelength of the radiation itself. For example, an intensity acquisition chain with 100 ps time-resolution requires an OPD control with millimetric accuracy only. Moreover, the link between individual telescopes only involves signal cables and no optical delay lines. In addition, the role of the telescopes is only to collect photons onto the sensitive surfaces of the sensors. This requires correct guiding and if possible fast tip-tilt correction, but the optical quality of the telescopes can be less-than-ideal. Besides, as emphasized by Tan et al (2016), operation is still possible in real conditions, that is, through atmospheric turbulence and even with some sky background contamination (full Moon).

Intensity interferometry is thus much easier to implement, especially with long baselines and is less sensitive to optical defects and atmospheric turbulence. However, it suffers from a lack of sensitivity (Hanbury Brown, 1974), requiring large collecting areas. For this reason, intensity interferometry has not been developed further since the early 1970', until the last decade where a significant jump was performed by the technology of light detectors and signal digital correlators. Single photon avalanche diodes (SPAD) are now commercially available in the visible domain, with unprecedented sensitivity, short dead time and high time resolution. Moreover, time to digital converters (TDC) which can process the electric pulses delivered by SPADs with count rates as high as several Mcps (millions of counts per second) and time resolution of a few picoseconds are now also available. A review of commonly used SPADs and TDCs can be found in table 1 from Pilyavsky et al (2017). These recent technological advances shed a new light on intensity interferometry for astronomy. For this reason, and despite its lack of sensitivity, intensity interferometry is now considered as a possible alternative to standard amplitude interferometry for very long baselines (kilometric and more) in the visible and near infrared domain.

This solution has been proposed as an alternative observing mode for the future Cherenkov Telescope Array (LeBohec and Holder, 2006; Nuñez et al, 2012; Dravins et al, 2013). With several tens of 4 m to 23 m telescopes spread over kilometric-sized areas, this facility will offer an unprecedented photon collecting area with sub-milliarcsecond angular resolutions and dense (u, v) plane coverage. However, these telescopes are not designed to be diffraction-limited and have a very large aperture ratios. This is likely to introduce technical difficulties to couple the telescopes with the photon detection devices.

Another approach to revive intensity interferometry methods is to implement it on existing diffraction-limited optical telescopes. This is the strategy followed for example by the "Asiago group" (Capraro et al, 2010; Zampieri et al, 2016). They have implemented intensity interferometry on the Copernicus and Galileo telescopes in Asiago (1.82 m and 1.22 m respectively), coupled with the cutting edge high velocity and high efficiency photon-counting photometers "Aqueye+" and "Iqueye" (Naletto et al, 2009).

In 2017, Pilyavsky *et al.* conducted extensive numerical simulations of intensity interferometry on seven 0.9 m to 4.0 m telescopes at Kitt Peak observatory (Pilyavsky et al, 2017). Their simulations suggest that valuable science throughput on stellar diameters of hot stars can be achieved with commercially available components and without excessive technical complexity.

This renewal of interest around intensity interferometry has led our research team to conduct new experiments with state-of-the-art avalanche photodiodes and time-to-digital converters. In 2016, we had performed laboratory experiments with artificial light sources (Dussaux et al, 2016), to assess the capability of our setup to detect the photon bunching phenomenon. In this article, we describe further experiments we have conducted in 2017 on bright stars with one, then with two 1 m telescopes. We also discuss further more ambitious experiments that we plan to perform in a near future. We finally

present possible implementations of these techniques on existing arrays of telescopes.

2 From amplitude to intensity interferometry on the French Riviera

Following the pioneer optical long baseline interferometers on the French Riviera (Labeyrie, 1975; Labeyrie et al, 1986) and given our currently operating focal instruments (VEGA-CHARA at Mount Wilson (Mourard et al, 2015) and AMBER at Paranal ESO-VLTI (Petrov et al, 2007) or MATISSE (Lopez et al, 2014), recently commissioned), we have initiated pilot experiments in 2015, aimed at attempting intensity interferometry in the visible and the near infrared using the two 1 meter optical telescopes of the C2PU facility (<https://www.oca.eu/index.php/fr/accueil-c2pu>) in view of implementing this technique on future arrays of optical telescopes. The C2PU facility is located at the Calern observing site of the *Observatoire de la Côte d’Azur* (hereafter OCA). We call this project “I2C” for Intensity Interferometry at Calern. I2C follows a stepwise approach to validate the focal instrument concept and components, including analysis and interpretation methods, and to reliably estimate the achievable sensitivity.

Like other groups, we have considered application to Cerenkov arrays which can be used for intensity interferometry during bright time, especially CTA for its photon-collecting surface which is almost equivalent to a 100 m dish with a maximum baseline of 2500 m, once the array is completed. However the angular spread of a Cerenkov telescope focal image is large, so that the light can only poorly be coupled to a single multimode fiber. Also, the sky background photon noise, integrated over the entire Cerenkov telescope angular spread, will affect the limiting magnitude. It is possible to introduce optical components to correct for the Cerenkov telescope primary mirror aberrations, but this dramatically complicates the design and complexity of these arrays primarily dedicated to high energy astrophysics. Another possible approach would be to use large surface detectors such as photomultipliers (Matthews et al, 2017), at the expense of a lower electronic bandpass, therefore lower intrinsic setup visibility.

Our technical choice is based on optical fibers connected to SPADs rather than photomultipliers. So, there are advantages to using existing optical telescopes to implement intensity interferometry techniques. Optical telescopes, whatever their size, generally provide seeing limited focal images, so that stellar photons can be transported by optical fibers to photon-counting detectors in order to estimate the intensity correlation function $g^2(\tau, \rho)$ defined by :

$$g^{(2)}(\tau, \rho) = \frac{\langle I(t, r)I(t + \tau, r + \rho) \rangle}{\langle I(t, r) \rangle^2}. \quad (1)$$

With seeing-limited telescopes, at least 50% coupling efficiencies are achievable with multimode optical fibers, which are cheap and commercially available.

However, the very narrow bandpass required to preserve coherence of the photons implies that a large fraction of the light is rejected and not used in the correlation measurements. Therefore as already noted by Hanbury Brown (1974), the most promising way to significantly improve the instrumental sensitivity of intensity interferometry is to observe spectrally dispersed light from the source with multiple photodetectors simultaneously at different wavelengths *i.e.*, multiple spectral channels. Besides accessing valuable spectral lines to probe stellar surfaces and circumstellar structures, triggered by magnetic fields, mass loss or colliding winds, there is also gain on the intrinsic instrumental contrast, and hence the signal-to-noise ratio (SNR), which improves as the square root of the spectral channels simultaneously correlated (Trippe et al, 2014).

To keep the volume and design of a high dispersion spectrograph reasonable, it is much preferable to use single mode (SM) fibers, which allow the use of fibered Fabry-Pérot etalons, fibered Bragg gratings or integrated (on-chip) spectrograph technology, to work on a large number of simultaneous narrow band spectral channels. To couple the light into SM fibers, the telescopes must be equipped with adaptive optics; however, the optical throughput and the decreasing Strehl ratio at short wavelengths can negatively affect the sensitivity, and a trade study is required to compare different SM coupling technologies, such as photonics lanterns. These can be used to split the light into a number of SM fibers, which can then each be dispersed spectrally. The output of all the SM fibers can then be co-added before or after detection of each spectral channel.

2.1 Results from temporal bunching at C2PU

On the nights of February 20, 21, and 22, 2017, we have measured (Guerin et al, 2017) what we believe to be the first intensity correlation measured with the light of a star other than the sun (Tan et al, 2014) since HBT historical experiments. The temporal photon bunching $g^{(2)}(\tau, r = 0)$, obtained in the photon counting regime, was measured for 3 bright stars, α Boo, α CMi, and β Gem. The light was collected at the focal plane of the West telescope of the C2PU facility (IAU observatory code: 010, latitude: $43^\circ 45' 13''$ N, longitude: $06^\circ 55' 22''$ E, altitude: 1270 m). The instrument is a $F/12.5$ pure Cassegrain combination, but to improve the fiber coupling efficiency, we have reduced the focal ratio to $F/5.6$ by inserting a combination of commercially available focal reducers. In the resulting focal plane, we have placed our compact optical setup. It consists of a dichroic beam splitter, a CCD guiding camera, a combination of filters and a multi-mode fiber (see Fig. 1 in Guerin et al (2017)). The light reflected by the dichroic ($\lambda < 650$ nm) is sent to the guiding camera. The transmitted light goes through a linear polarizer, then through two cascaded narrow band dielectric filters centered on $\lambda_0 = 780$ nm. The resulting bandwidth is 1 nm with a throughput estimated as 61% for the central wavelength.

Table 1 Main data and results of temporal bunching on the three stars observed in February 2017 at C2PU. T is the total integration time, in hours and minutes. The flux \mathcal{F} is the number of detected photon counts per second and per detector, averaged over the total integration time. The contrast $\mathcal{C} = g^{(2)}(0) - 1$ is the value of the correlation at zero delay given by the amplitude of the Gaussian fit, its uncertainty is the 1σ confidence interval of the fit. The noise is the *rms* noise on the data evaluated in the wings of the correlation function, where $g^{(2)}(\tau) \simeq 1$.

Star	Sp. type	R mag	I mag	T	$\mathcal{F} (\times 10^6)$	$\mathcal{C} (\times 10^{-3})$	noise $(\times 10^{-3})$
α Boo	K0-III C	-1.03	-1.68	1:55'	2.29	1.81 ± 0.19	0.32
α CMi	F5IV-V	-0.05	-0.28	4:35'	1.44	1.90 ± 0.28	0.46
β Gem	K0-III	+0.39	-0.11	6:50'	0.85	2.38 ± 0.43	0.78

The light is then transported by a 20 m-long multimode graded-index fiber (MMF) with a core diameter of $100 \mu\text{m}$, which is connected to a 50:50 fibered splitter such that two photodetectors can be used to compute the autocorrelation function without being limited by the dead time of the detectors, which is much larger than the coherence times. The two output ports of the splitter are connected to SPADs via two other MMFs of 1 m for the first detection channel and 2 m for the second. In order to avoid any spurious correlation induced by electronic cross-talk, we have introduced an electronic delay between the two channels by using a 10 m shielded BNC cable for the second channel and 1 m for the first channel. The total delay (optical and electronic) between the two channels is $t_0 \simeq 45$ ns and is subtracted in the data processing. For each detected photon, the SPADs produce a 10 ns pulse, whose rising edge is detected and processed by a TDC with a time bin of 162 ps. The TDC is operated in the ‘‘Delay-Histogram’’ mode, which yields a good approximation of the intensity correlation function after proper normalization.

For total exposure times of a few hours, we obtained contrast values around 2×10^{-3} (see Table 1), in agreement with the theoretical expectation for chaotic sources, given the optical and electronic bandwidths of our setup. Figure 1 displays a typical correlation graph ($g^{(2)}(\tau)$ vs τ) obtained on the star α Boo (Arcturus).

It is worth comparing the performances of our measurements with the Narrabri intensity interferometry results published by Hanbury Brown et al (1967b). For this sake, we can use the star α CMi, which has been observed by both instruments. For the Narrabri instrument, the contrast of the correlation measured with the shortest baseline is reported with a SNR of 11.5 for a 13.9 hours observing time. We obtained a SNR of 6.8 with only 4.6 hours observing time and with a collecting area approximately 85 times smaller (the Narrabri interferometer used two 6.5 m collectors, whilst we used a single 1 m telescope with 9.7% central obscuration). The improvement in performance is due to the larger electronic bandwidth, the better quantum efficiency of the detectors, the fact that there are no correlation losses due to the separation of the telescopes (the minimal baseline of the Narrabri interferometer was 9.5 m) and our working wavelength of 780 nm, which is more adapted to the spectral type (F5IV) of α CMi than Narrabri’s wavelength (443 nm). Moreover, the

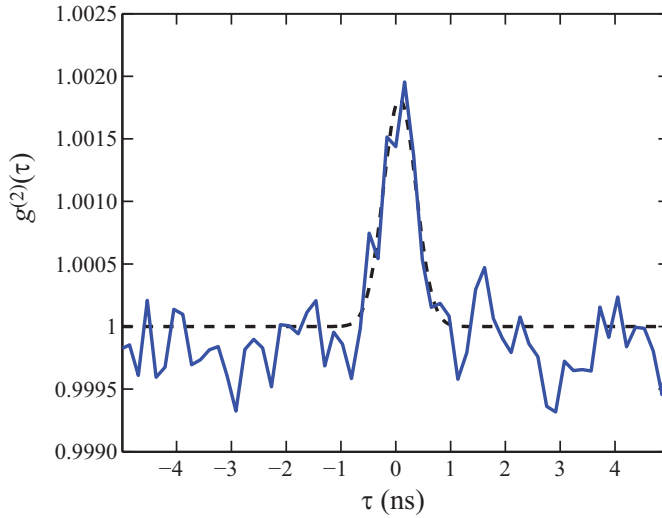


Fig. 1 Temporal intensity correlation function $g_g^{(2)}(\tau, r = 0)$ measured on α Boo (Arcturus) in February 2017. The Gaussian fit (dashed line) is used to estimate the contrast (reported in Table 1) and the FWHM of the bunching peak. The fit window is $[-10, 10]$ ns.

performances of the system used by Guerin et al (2017) can be improved in two ways. First, a faster TDC and/or the choice of the “photon time tagging” mode, associated to an appropriate data post-processing system, allow for improved measurements of the correlation function. Second, we can increase the efficiency of our telescope-to-fiber coupling strategy by introducing a fast tip-tilt correction stage or, preferably, a low-order adaptive optics.

2.2 Preliminary results from spatial bunching

The transition from the temporal bunching experiments of February 2017 (Guerin et al, 2017) to spatial bunching observations has been quite fast and the first successful observations were performed in October 2017. The presence in the same facility (C2PU) of two independent but nearly identical 1 m telescopes, separated by 15 m has made this evolution relatively easy. For this, the fibered splitter used to feed both SPADs from the flux of a single telescope was removed. Instead, two optical fibers coming from both telescopes were connected to the two SPADs. So, our telescope-to-fiber coupling system has been duplicated (same guiding camera, same set of filters) and both replicas were set in the focal planes of the two telescopes.

Three bright stars (α Lyr, β Ori and α Aur) were observed during 4 nights, from 10th to 13th October 2017. The correlation peak emerged easily, provided a suitable delay be taken into account (connection wire lengths difference and time-dependent astronomical optical path difference). Fig. 2 depicts the correlation peak detected on α Lyr for a total of 11.1 hours integration time

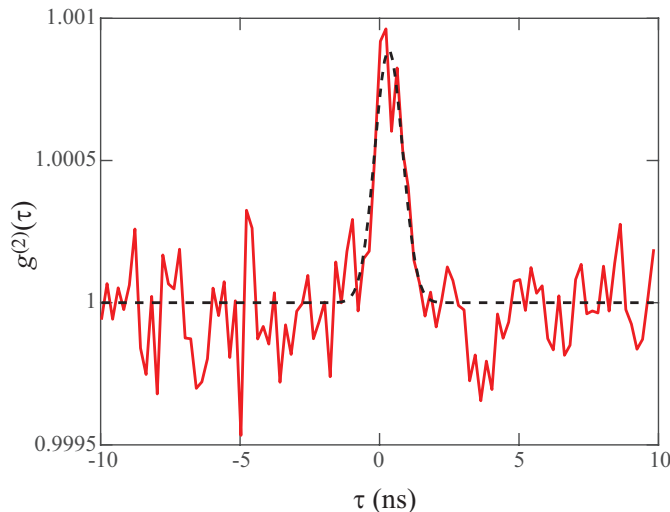


Fig. 2 Spatial intensity correlation function $g^{(2)}(\tau, r)$ measured for α Lyr in October 2017. The Gaussian fit (dark solid line) is used to extract the contrast and the FWHM of the bunching peak. The fit window is $[-10, 10]$ ns.

spread over 3 nights. The on-sky projected baseline ranged from 9.6 m to 14.3 m, with a time-averaged value of 11.9 m. The contrast was measured as $(0.89 \pm .09) \times 10^{-3}$ ($1\text{-}\sigma$ uncertainty, *i.e.* SNR= 10). Taking into account the temporal resolution of the detection chain, this value is quite consistent with the known value of the uniform disk angular diameter of α Lyr (3.14 mas), taking into account a 11.9 m projected baseline. A more detailed study on other bright stars is under progress and will be presented in a forthcoming detailed paper.

2.3 The I2C project : future developments

Following the straightforward success of intensity interferometry techniques on the C2PU facility at OCA, we have initiated a short term plan to overcome its limitations and to improve its robustness for a further deployment on larger facilities in other observatories (see Sect. 3). The immediate plan is to improve our prototype experiment sub-system components to gain on the sensitivity (limiting coherent magnitude, *i.e.* source apparent brightness and effective visibility) whilst comparing its performances to operating optical direct interferometers like CHARA and/or NPOI through stellar sources with accurate angular diameters.

A first step is based on introducing polarization beam-splitters to observe stars with extended atmospheres and/or wind envelopes simultaneously in two polarizations, parallel and perpendicular to the interferometric baseline. HBT's early observations at Narrabri on Rigel (Hanbury Brown et al, 1974b)

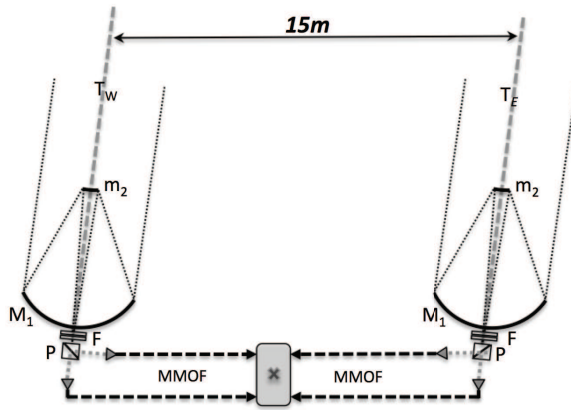


Fig. 3 Optical configuration of the I2C interferometer at OCA for stellar polarization and/or differential angular diameter measurements in the continuum versus emission lines such as $H\alpha$. T_W and T_E are respectively the West and East 1 m optical telescopes of the C2PU facility. M_1 and m_2 are the primary and secondary mirrors (both telescopes have nearly identical optical combinations). Seeing limited images at the Cassegrain secondary foci are split in their two linearly polarized components and injected into two separate multimode optical fibers (MMOF), which transport the corresponding lights to SPADs. All four SPADs are connected to four input ports of the correlator X . Here, each polarization from both telescope is correlated to its counterpart from the other telescope so that $g^{(2)}(\tau, r)$ estimates are obtained simultaneously in polarized light parallel and perpendicular to the baseline. For C2PU the maximum East-West baseline reaches 15 m, corresponding to an angular resolution of 9.6 mas at 700 nm. Note that F are 1 nm bandwidth filters either centered on $H\alpha$ line or at the 780 nm continuum to achieve differential visibility measurements.

have proven that substantial gains in accuracy on the visibility are required to measure any deviation from the uniform disk model, according to realistic stellar atmosphere models of early type stars (Cassinelli and Hoffman, 1975). Since then, direct interferometers have been unsuccessful to achieve such measures (Vakili, 1981) due to instrumental polarization effects (*e.g.* time-varying oblique reflections and cross-talk) introduced by the optical complexity of amplitude interferometers. Intensity interferometry is immune by construction to such effects since one can directly separate two polarizations and correlate them independently without any loss in SNR. Moreover, a gain of $\sqrt{2}$ is expected for unpolarized sources, by co-adding the correlation functions of both polarization states.

Fig. 3 depicts the generic configuration of the I2C interferometer project. This layout also allows to observe differential effects between two spectral channels (one in the continuum and one on some emission lines such as $H\alpha$). This is interesting for hot stars, for instance Be or LBV like γ Cas or P Cyg, which have been formerly observed in amplitude interferometry at OCA (Vakili et al, 1997).

A second step consists in increasing the angular resolution by performing intensity correlation experiments involving one or two telescopes from C2PU and one telescope of the “MeO” laser-ranging facility (Samain, 2015), located

at 150 m of the C2PU building. Synchronization between these distant telescopes can be achieved via cable or fiber connection with adequate control or measurement of transmission delays.

Most modern TDCs can be used in two modes : cross-correlation computation and photon time-tagging mode. Both modes can be used for astronomical intensity interferometry. If the electric signals of two (or more) SPADs linked to two (or more) telescopes, are fed into two (or more) channels of the same TDC via coaxial cables, then the cross-correlation computation mode will deliver directly the photon arrival time correlation function with a time delay which needs to be computed and specified *a priori*. This operating mode requires a physical connection between telescopes through cables. On the contrary, if each telescope has its own SPAD, its own TDC (set in time-tagging mode), which delivers its time-tagging strings to its own computer, then no physical link is required between the telescopes. Correlations can be computed numerically afterwards. Of course, all TDCs need to be accurately synchronized to a common time reference (*e.g.* UTC). This configuration is more expensive but more straightforward to extrapolate to very long baselines, since no physical connection is required. Another advantage is that the correlation functions can be computed numerically *a posteriori* from the sets of photon arrival times, recorded independently by different TDCs and stored on independent mass storage devices. Contrary to correlations computed “on the fly” during the observation run, *a posteriori* correlations computation allows for more elaborate algorithms, for example with time-varying and/or adjustable parameters. This configuration with no physical link between telescopes could be tested as a third step of our experiment. In our case, the necessary time reference for the TDCs would be provided by the local time standard of the “MeO” instrument. This time standard offers a temporal resolution and stability on the order of a few picoseconds, which is significantly better than the coherence length of our intensity correlation measurements (of the order of 3 cm, because of the time-resolution of our SPADs).

Finally, we are also considering 3-telescope intensity correlation experiments between the two C2PU 1 m telescopes and the MeO laser-ranging 1.5 m telescope. The West-North-West direction of MeO with respect to C2PU offers much longer projected baselines than C2PU itself. They range between a few tens of meters and 150 m depending on the target’s position. This leads to sub-mas resolutions for visible wavelengths (*e.g.* in the range of 600-800 nm). Indeed, triple correlations between 3 telescopes would provide the closure phase quantity (Malvimat et al, 2014) but at the expense of a much higher exposure time for a given SNR. Several hundreds hours of integration would be necessary with the aforementioned OCA telescopes to attain the SNR value required to access any measure of phase information from the triple correlation quantity. However the power of intensity interferometry, despite its intrinsic low SNR and sensitivity, lies in the fact that the correlation signal can be integrated over many nights since no fringe detection or tracking is necessary as in amplitude interferometry.

Table 2 Potential arrays of optical telescopes with the highest photon-collecting surfaces and kilometeric baselines suitable for modern intensity interferometry. N_T is the number of telescopes with diameters larger than 1.5 m, S is the total collecting surface of the array in m^2 (assuming 10% to 15% losses due to the central obstruction), N_b is the number of possible array baselines, B_m is the array theoretical maximum baseline in meters and ρ the potential angular resolution in mas at 700 nm wavelength. Last column gives the potential photon collecting area and/or the longest baseline becoming available if extremely large telescopes are built at or close to the corresponding observing sites.

Observatory	N_T	S	N_b	B_m	ρ	Comment
ESO Paranal	8	220	28	220	0.7	1200 m^2 and 21 km with ELT
Mauna Kea	8	260	28	2500	0.06	1260 m^2 with TMT
La Palma	4	100	6	1200	0.12	1100 m^2 with TMT

3 Prospects and discussion

The revival of intensity interferometry half a century after the pioneering work by Hanbury Brown and Twiss suggests that these techniques are promised to open new opportunities for very high angular resolution observations in the future, specially in the visible wavelengths, down to the violet if the site transparency permits. Two approaches have been proposed until now: the first one is based upon the use of existing or foreseen Cerenkov telescope arrays (Dravins and LeBohec, 2008; Matthews et al, 2017), and the second one is to use existing seeing limited optical telescopes (Zampieri et al, 2016; Pilyavsky et al, 2017; Guerin et al, 2017). Simulations and laboratory experiments confirm the imaging potential of HBT arrays whatever Cerenkov or optical. We started and effectively demonstrated that photon bunching, either temporal or spatial can be straightforwardly achieved with two modest 1 m telescopes at OCA using almost “off-the-shelf” quantum optics photonic components, at least if instrumental effects are correctly controlled and calibrated. As argued by Trippe et al (2014), multichannel correlations, with hundreds of simultaneous narrow spectral channels, is the most promising way to progress over the intrinsic limitations of intensity interferometry for a given limited number and photon collecting surface. Much experience is to be gained however by using existing 1-2 m class telescopes, coupled later to 8-10 m class telescopes for on-sky observations in order to control the detailed behavior of photonic subsystems and components of an intensity interferometer on various astrophysical sources before speculating on the observation of exotic or extragalactic sources with microarcsecond angular resolutions. Considering this, we propose to consider intensity interferometry on a few major observatories (see Table 2) and a first prototype HBT array based on the four 1.8 m ATs at Paranal/Chile (A. Mérand, private communication) that would be available for such experiments and observations when the VLTI focal instruments MATISSE and GRAVITY occupy the Paranal optical delay lines.

Acknowledgements The I2C pilot experiment is supported by INPHYNI and Lagrange laboratories, Döblin Federation and grants from OCA and the Excellence Initiative UCA-JEDI from University Côte d’Azur. We are grateful to A. Dussaux for his valuable contri-

bution to this project. We also thank E. Samain, C. Courde and J. Chabé (GeoAzur lab., OCA) for fruitful discussions about space and time metrology. Ph. Bério from Lagrange Laboratory (OCA) is also kindly acknowledged.

References

- Capraro I, Barbieri C, Naletto G, Occhipinti T, Verroi E, Zoccarato P, , Gradari S (2010) Quantum astronomy with Iqueye. *Proc SPIE* 7702:77,020M
- Cassinelli JP, Hoffman NM (1975) The effect of linearly polarized light from extended stellar atmospheres on interferometer response functions. *MNRAS* 173:789–800
- Dravins D, LeBohec S (2008) Toward a diffraction-limited square-kilometer optical telescope: digital revival of intensity interferometry. *Proc SPIE* 6986:698,609
- Dravins D, LeBohec S, Jensen H, Nuñez PD (2013) Optical intensity interferometry with the Cherenkov Telescope Array. *Astropart Phys* 43:331–447
- Dussaux A, Passerat de Silans T, Guerin W, Alibart O, Tanzilli S, Vakili F, Kaiser R (2016) Temporal intensity correlation of light scattered by a hot atomic vapor. *Phys Rev A* 93:043,826
- Garcia EV, Muterspaugh MW, van Belle G, Monnier JD, Stassun KG, Ghasempour A, Clark JH, Zavala RT, Benson JA, Hutter DJ, et al (2016) VISION: A Six-telescope Fiber-fed Visible Light Beam Combiner for the Navy Precision Optical Interferometer. *PASP* 128:055004
- Gomes N, Garcia PJV, Thiébaud E (2017) Assessing the quality of restored images in optical long-baseline interferometry. *MNRAS* 465:3823–3839
- Guerin W, Dussaux A, Fouché M, Labeyrie G, Rivet JP, Vernet D, Vakili F, Kaiser R (2017) Temporal intensity interferometry: photon bunching in three bright stars. *MNRAS* 472:4126–4132
- Hanbury Brown R (1968) Stellar interferometer at Narrabri observatory. *Nature* 218:637–641
- Hanbury Brown R (1974) *The intensity interferometer: Its application to astronomy*. Taylor and Francis, Ltd
- Hanbury Brown R, Twiss RQ (1956a) Correlation between photons in two coherent beams of light. *Nature* 177:27–29
- Hanbury Brown R, Twiss RQ (1956b) A test of a new type of stellar interferometer on Sirius. *Nature* 178:1046–1048
- Hanbury Brown R, Jennison RC, Gupta MKD (1952) Apparent angular sizes of discrete radio sources: Observations at Jodrell Bank, Manchester. *Nature* 170:1061–1063
- Hanbury Brown R, Davis J, Allen LR (1967a) The stellar interferometer at Narrabri observatory – I. *MNRAS* 137:375–392
- Hanbury Brown R, Davis J, Allen LR, Rome JM (1967b) The stellar interferometer at Narrabri observatory – II. *MNRAS* 137:393–417
- Hanbury Brown R, Davis J, Allen LR (1974a) The angular diameters of 32 stars. *MNRAS* 167:121–136

- Hanbury Brown R, Davis J, Allen LR (1974b) An attempt to detect a corona around beta Orionis with an intensity interferometer using linearly polarized light. *MNRAS* 168:93–100
- Labeyrie A (1975) Interference fringes obtained on Vega with two optical telescopes. *ApJ* 196:L71–L75
- Labeyrie A, Schumacher G, Dugué M, Thom C, Bourlon P (1986) Fringes obtained with the large ‘boules’ interferometer at CERGA. *A&A* 162:359–364
- LeBohec S, Holder J (2006) Optical intensity interferometry with atmospheric Cherenkov telescope array. *ApJ* 649:399–405
- Lopez B, Lagarde S, Jaffe W, Petrov R, Schöller M, Antonelli P, Beckman U, Berio P, Bettonvil F, Graser U, et al (2014) MATISSE status report and science forecast. *Proc SPIE* 9146:91,460Z
- Malvimat V, Wucknitz O, Saha P (2014) Intensity interferometry with more than two detectors? *MNRAS* 437:798–803
- Matthews N, Kieda D, LeBohec S (2017) Development of a digital astronomical intensity interferometer: laboratory results with thermal light. *J Mod Opt* 65:1336–1344
- Mills BY (1952) Apparent angular sizes of discrete radio sources: Observations at Sydney. *Nature* 170:1063–1064
- Mourard D, Monnier JD, Meilland A, Gies D, Millour F, Benisty M, Che X, Grundstrom ED, Ligi R, Schaefer G, et al (2015) Spectral and spatial imaging of the Be+sdO binary ϕ Persei. *A&A* 577:A51
- Naletto G, Barbieri C, Occhipinti T, Capraro I, Di Paola A, Facchinetti C, Verroi E, Zoccarato P, Anzolin G, Belluso M, et al (2009) Iqueye, a single photon-counting photometer applied to the ESO new technology telescope. *A&A* 508:531–539
- Nuñez PD, Holmes R, Kieda D, LeBohec S (2012) High angular resolution imaging with stellar intensity interferometry using air Cherenkov telescope array. *MNRAS* 419:172–183
- Petrov RG, Malbet F, Weigelt G, Antonelli P, Beckmann U, Bresson Y, Chelli A, Dugué M, Duvert G, Gennari S, Glück L, Kern P, Lagarde S, Le Coarer E, Lisi F, Millour F, Perraut K, Puget P, Rantakyro F, et al (2007) AMBER, the near-infrared spectro-interferometric three-telescope VLTI instrument. *A&A* 464:1–12
- Pilyavsky G, Mausekopf P, Smith N, Schroeder E, Sinclair A, van Belle GT, Hinkel N, Scowen P (2017) Single-photon intensity interferometry (SPIIFy): utilizing available telescopes. *MNRAS* 467:3048–3055
- Samain E (2015) Clock comparison based on laser ranging technologies. *Int J Mod Phys D* 24:1530,021
- Smith FG (1952) Apparent angular sizes of discrete radio sources: Observations at Cambridge. *Nature* 170:1065
- Tan PK, Yeo GH, Poh HS, Chan AH, Kurtsiefer C (2014) Measuring temporal photon bunching in backbody radiation. *ApJ* 789:L10
- Tan PK, Chan AH, Kurtsiefer C (2016) Optical intensity interferometry through atmospheric turbulence. *MNRAS* 457:4291

-
- Trippe S, Kim JY, Lee B, Choi C, Oh J, Lee T, Yoon SC, Im M, Park YS (2014) Optical multi-channel intensity interferometry – or : How to resolve O-stars in the Magellanic clouds. *Journal of the Korean Astronomical Society* 47:235–253
- Vakili F (1981) Study of stellar polarization with the CERGA interferometer. *A&A* 101:352–355
- Vakili F, Mourard D, Bonneau D, Stee P (1997) Subtle structures in the wind of P Cygni. *A&A* 323:183–188
- Zampieri L, Naletto G, Barbieri C, Barbieri M, Verroi E, Umbriaco G, Favazza P, Lessio L, Farisato G (2016) Intensity interferometry with Aqueye+ and Iqueye in Asiago. *Proc SPIE* 9907:99,070N